Tackling Variability: A Multicenter Study to Provide a Gold-Standard Network Approach for Frontotemporal Dementia

Lucas Sedeño,[1,2] Olivier Piguet,[3,4] Sofía Abrevaya,[1,2] Horacio Desmaras,[1] Indira García-Cordero,[1,2] Sandra Baez,[1,2,5] Laura Alethia de la Fuente,[1,2] Pablo Reyes,[6] Sicong Tu,[7,8,9] Sebastian Mogilner,[1,10,11] Nicolas Lori,[1,12,13,14] Ramon Landin-Romero,[3,4] Diana Matallana,[6] Andrea Slachevsky,[15,16,17,18] Teresa Torralva,[1] Dante Chialvo,[2,19] Fiona Kumfor,[3,4] Adolfo M. García,[1,2,20] Facundo Manes,[1,2,9] John R Hodges,[3,4] and Agustin Ibanez [1,2,9,21,22]*

[1]Institute of Cognitive and Translational Neuroscience (INCyT), INECO Foundation, Favaloro University, Buenos Aires, Argentina
[2]National Scientific and Technical Research Council (CONICET), Buenos Aires, Argentina
[3]Neuroscience Research Australia, Sydney, Australia and School of Medical Sciences, The University of New South Wales, Sydney, Australia
[4]School of Psychology, Central Clinical School & Brain and Mind Centre, University of Sydney; Neuroscience Research Australia; ARC Centre of Excellence in Cognition and its Disorders, New South Wales, Australia
[5]Universidad de los Andes, Bogota, Colombia
[6]Intellectus Memory and Cognition Center, Mental Health and Psychiatry Department, Hospital Universitario San Ignacio, Pontificia Universidad Javeriana, Colombia
[7]FMRIB, Nuffield Department of Clinical Neurosciences, Oxford University, Oxford, United Kingdom
[8]Brain and Mind Centre, Sydney Medical School, University of Sydney, Sydney, Australia
[9]Australian Research Council Centre of Excellence in Cognition and its Disorders, Sydney, Australia
[10]Fundación Escuela de Medicina Nuclear (FUESMEN) and Comisión Nacional de Energía Atómica (CNEA), Buenos Aires, Argentina
[11]Instituto Balseiro and Facultad de Ciencias Exactas y Naturales, Universidad Nacional de Cuyo (UNCuyo), Mendoza, Argentina

Additional Supporting Information may be found in the online version of this article.

Conflict of interest: The authors declare no conflict of interest.
Contract grant sponsor: CONICYT/FONDECYT Regular; Contract grant number: (1170010), PICT 2012-0412, PICT 2012-1309, CONICET, CONICYT/FONDAP 15150012 and the INECO Foundation; Contract grant sponsor: a National Health and Medical Research Council of Australia (NHMRC) Research Project Grant; Contract grant number: 510106; Contract grant sponsor: ForeFront, a collaborative research group dedicated to the study of frontotemporal dementia and motor neuron disease, from the NHMRC; Contract grant number: APP1037746; Contract grant sponsor: Australia Research Council (ARC) Centre of Excellence in Cognition and its Disorders Memory Node; Contract grant number: CE11000102; Contract grant sponsor: FK is supported by an NHMRC-ARC Dementia Research Development Fellowship; Contract grant number: APP1097026; Contract grant sponsor: OP is supported by an NHMRC Senior Research Fellowship; Contract grant number: APP1103258; Contract grant sponsor: ST is supported by an NHMRC Early Career Research Fellowship; Contract grant number: APP1121859; Contract grant sponsor: PR and DM are supported by the Grant Colciencias; Contract grant number: 697-2014.

*Correspondence to: Agustin Ibanez, Pacheco de Melo 1860, C1126AAB, Buenos Aires, Argentina. E-mail: aibanez@ineco.org.ar

Received for publication 26 January 2017; Revised 29 March 2017; Accepted 17 April 2017.
DOI: 10.1002/hbm.23627
Published online 00 Month 2017 in Wiley Online Library (wileyonlinelibrary.com).

[12]INECO Neurociencias Oroño, Grupo Oroño, Rosario, Argentina
[13]Centro Algoritmi, University of Minho, Guimarães, Portugal
[14]Laboratory of Neuroimaging and Neuroscience (LANEN), INECO Foundation Rosario, Rosario, Argentina
[15]Physiopathology Department, ICBM Neuroscience Department, Faculty of Medicine, University of Chile, Santiago, Chile
[16]Cognitive Neurology and Dementia, Neurology Department, Hospital del Salvador, Providencia, Santiago, Chile
[17]Gerosciences Center for Brain Health and Metabolism, Santiago, Chile
[18]Centre for Advanced Research in Education, Santiago, Chile
[19]Center for Complex Systems & Brain Sciences - Escuela de Ciencia y Tecnologia. UNSAM/Campus Miguelete, Argentina
[20]Faculty of Education, National University of Cuyo (UNCuyo), Mendoza, Argentina
[21]Universidad Autonoma del Caribe, Barranquilla, Colombia
[22]Center for Social and Cognitive Neuroscience (CSCN), School of Psychology, Universidad Adolfo Ibañez, Santiago, Chile

Abstract: Biomarkers represent a critical research area in neurodegeneration disease as they can contribute to studying potential disease-modifying agents, fostering timely therapeutic interventions, and alleviating associated financial costs. Functional connectivity (FC) analysis represents a promising approach to identify early biomarkers in specific diseases. Yet, virtually no study has tested whether potential FC biomarkers prove to be reliable and reproducible across different centers. As such, their implementation remains uncertain due to multiple sources of variability across studies: the numerous international centers capable conducting FC research vary in their scanning equipment and their samples' socio-cultural background, and, more troublingly still, no gold-standard method exists to analyze FC. In this unprecedented study, we aim to address both issues by performing the first multicenter FC research in the behavioral-variant frontotemporal dementia (bvFTD), and by assessing multiple FC approaches to propose a gold-standard method for analysis. We enrolled 52 bvFTD patients and 60 controls from three international clinics (with different fMRI recording parameters), and three additional neurological patient groups. To evaluate FC, we focused on seed analysis, inter-regional connectivity, and several graph-theory approaches. Only graph-theory analysis, based on weighted-matrices, yielded consistent differences between bvFTD and controls across centers. Also, graph metrics robustly discriminated bvFTD from the other neurological conditions. The consistency of our findings across heterogeneous contexts highlights graph-theory as a potential gold-standard approach for brain network analysis in bvFTD. *Hum Brain Mapp 00:000–000, 2017.*

Key words: biomarkers; frontotemporal dementia; functional connectivity; graph-theory and neurodegenerative diseases

INTRODUCTION

Multiple research efforts aim to detect sensitive early biomarkers for neurodegenerative diseases, as these can contribute to studying potential disease-modifying agents, fostering timely therapeutic interventions, and alleviating associated financial costs (Henley et al., 2005; Humpel, 2011; Shaw et al., 2007). Functional connectivity (FC) analysis represents a promising approach in this context (Pievani et al., 2011, 2014). Yet, virtually no study has tested whether potential FC biomarkers prove to be reliable and reproducible across different centers. As such, their implementation remains uncertain due to multiple sources of variability across studies. First, the numerous international centers capable of conducting FC research vary in their scanning equipment and their samples' socio-cultural background; and second, while there are multiple approaches to derive FC measures (Pievani et al., 2011; van Wijk et al., 2010), no gold-standard method exists to analyze the data. These limitations undermine the reliability and reproducibility of FC results, which are essential requisites to be met by a candidate biomarker (Henley et al., 2005; Humpel, 2011). Here, we aim to address these

issues by performing an unprecedented multicenter FC analysis in the behavioral variant of the frontotemporal dementia (bvFTD), and by assessing multiple FC approaches to propose a gold-standard method for analysis.

FTD is the second most common dementia in patients below age 65 (Piguet et al., 2011a). Its relatively young onset, its clinical overlap with other diseases, and its variable pattern of brain atrophy make it difficult to achieve early diagnosis (Ibanez et al., 2014, Piguet et al., 2011a). Regarding FC, bvFTD patients consistently exhibit abnormalities in the salience network (SN), which encompasses the anterior cingulate cortex (ACC) as well as orbitofrontal and insular regions (Pievani et al., 2011, 2014). However, similar impairments have been documented in Alzheimer's disease (AD) (Pievani et al., 2014) and neuropsychiatric diseases (Menon, 2011). Moreover, research in genetic forms of presymptomatic bvFTD is inconclusive, reporting both absence of alterations (Whitwell et al., 2011) and changes (Dopper et al., 2014) of the SN. These results cast doubts on the preclinical sensitivity and specificity of SN disturbances as a hallmark of bvFTD. This controversy is further fueled by results from inter-regional connectivity analyzes (Zalesky et al., 2010), which evaluate the strength of connections between areas regardless of their encompassing resting-state network. In bvFTD, this method has shown both increased and decreased connectivity, even within the same area (e.g., insular cortex) (Agosta et al., 2013; Farb et al., 2013).

Arguably, discrepancies in the literature may reflect inconsistencies among MRI recording devices, measurement parameters, network analyzes, and even socio-demographic differences. To circumvent these limitations and look for specific biomarkers (Shaw et al., 2007), novel FC approaches must be tested across methodologically and socio-demographically heterogeneous settings. Crucially, most current proposals to assess FC fail to conceive the whole brain as a dynamic and interactive network (De Vico Fallani et al., 2014). A radically different viewpoint is offered by graph-theory, which allows characterizing the brain FC as a complex network of interconnected elements (Bullmore and Sporns, 2009; Sporns, 2014) with global and local properties. Promisingly, this method may afford powerful biomarkers of neurodegenerative disease (Pievani et al., 2011; Sporns, 2014). Yet, few graph-theory studies have demonstrated aberrant network organization in bvFTD (Agosta et al., 2013; Sedeno et al., 2016). This may be partially due to the lack of a gold-standard approach to derive graph measures from FC networks (Bullmore and Sporns, 2009; van Wijk et al., 2010).

Two outstanding questions thus emerge: (a) are any of the FC methods or graph-theory approaches robust enough to afford replicable findings across different fMRI acquisition contexts? (Papo et al., 2014; Shaw et al., 2007); and (b) can any of these measures reveal disorder-specific alterations? (Papo et al., 2014) This international multicenter study aims to address both questions by establishing a gold standard network-disruption signature of bvFTD. Specifically, we explored whether graph-theory compared to other FC methods (inter-regional connectivity and seed analysis) could robustly distinguish bvFTD patients from controls despite major variability in clinical diagnostic groups, fMRI parameters, and graph approaches. To this end, we enrolled participants from three international clinics specialized in neurodegeneration with different MRI scanners and acquisition parameters. Then, we compared diverse connectivity and graph-theory methods in the quest of systematic and sensitive network markers across countries. Finally, to evaluate our results' specificity, we replicated the study with three disease control groups: fronto-insular stroke (FIS), AD, and primary progressive aphasia (PPA).

MATERIALS AND METHODS

Participants

The study comprised 148 participants. Fifty-two patients fulfilling revised consensus criteria for probable bvFTD (Rascovsky et al., 2011) were recruited from three international clinics: INECO Foundation, Argentina (Country-1); San Ignacio University Hospital, Colombia (Country-2); and the frontotemporal dementia research group (FRONTIER) based at Neuroscience Research Australia, Australia (Country-3). As in previous reports (Baez et al., 2014; Piguet et al., 2011b; Torralva et al., 2009), clinical diagnosis in each center was established by a standard examination—including extensive neurological, neuropsychiatric, and neuropsychological assessments—and case revision by a multidisciplinary clinical meeting of bvFTD experts. The patients were functionally impaired and exhibited prominent changes in personality and social behavior, as verified by caregivers (behavioral features of bvFTD patients from each center are reported in Supporting Information Table S1). All patients showed frontal atrophy on MRI and frontal hypoperfusion (when SPECT were available). They were all in early/mild disease stages, did not fulfill criteria for specific psychiatric disorders, and they presented similar demographic features (Supporting Information Table S2). Patients presenting primarily with language deficits were excluded. As show in Table IA, each patient sample was matched on sex, age, and education with its own control group from the same scanning center. Healthy controls (sixty in total) presented no history of psychiatric or neurological disease.

To test the specificity of potential alterations in bvFTD, we recruited 13 Country-1 patients with FIS [a neurological condition with dissimilar pathophysiological mechanisms and different patterns of local-global connectivity (Garcia-Cordero et al., 2015)], and two other samples with neurodegeneration: 8 Country-2 patients fulfilling criteria for PPA (Gorno-Tempini et al., 2011), and 15 Country-3 patients who satisfied international criteria for AD (McKhann et al., 2011). FIS patients were evaluated at least six months post-stroke (to ensure stability of lesions and symptoms). These groups were sex-, age-, and education-matched with

TABLE I. Demographic and fMRI details

	Country-1: Argentina				Country-2: Colombia				Country-3: Australia			
A. Demographic characteristics of the study samples: Details of the comparison the groups of each center												
	C	bvFTD	FIS	Stats	C	bvFTD	PPA	Stats	C	bvFTD	AD	Stats
Number	16	16 (+5)	13	–	29	17	8	–	15	12 (+2)	13 (+2)	–
Age	63.50 (7.22)	69.37 (7.29)	62.77 (10.42)	NS	61.30 (7.16)	65.23 (8.29)	60.12 (5.81)	NS	69.13 (6.59)	65.33 (9.12)	64.07 (7.34)	NS
Educa-tion	16.31 (2.52)	14.60 (4.12)	14.25 (5.61)	NS	14.25 (5.60)	13.82 (4.50)	11.50 (4.37)	NS	14.15 (2.61)	12.10 (3.33)	12.77 (2.65)	NS
Gender	F = 9 M = 7	F = 9 M = 7	F = 3 M = 10	NS	F = 12 M = 17	F = 12 M = 5	F = 4 M = 4	NS	F = 7 M = 8	F = 8 M = 4	F = 5 M = 8	NS

B fMRI acquisition parameters: The specific scanning protocol followed in each center			
Firm	Philips Intera	Philips Achieva	Philips Achieva
Teslas	1.5 T	3 T	3 T
N° slices	33 slices	40 slices	29 slices
Voxel size	3.6 mm × 3.6 mm × 4 mm	3 mm × 3 mm × 3 mm	1.88 mm × 1.88 mm × 4.5 mm
Flip angle	90°	90°	90°
Acqui-sition	Ascending. Parallel to the anterior and posterior commissures.	Ascending. Parallel to the anterior and posterior commissures.	Ascending. Parallel to the anterior and posterior commissures.
Repe-tition time (TR)	2,777 ms	3,000 ms	2,000 ms
Echo time (TE)	50 ms	30 ms	30 ms
Duration	10 min	5 min	7 min
Instru-ction	"Do not think about anything in particular".	"Do not think about anything in particular".	"Do not think about anything in particular".
N° volumes	209	120	208

C Movement parameters: Comparison of groups' movement parameters in each center												
	C	bvFTD	FIS	Stats	C	bvFTD	PPA	Stats	C	bvFTD	AD	Stats
Mean translational (mm)	0.11 (0.05)	0.12 (0.07)	0.10 (0.03)	NS	0.05 (0.03)	0.05 (0.02)	0.05 (0.04)	NS	0.08 (0.04)	0.08 (0.03)	0.11 (0.07)	NS
Mean rotational (°)	0.07 (0.03)	0.09 (0.06)	0.08 (0.03)	NS	0.03 (0.01)	0.04 (0.02)	0.04 (0.02)	NS	0.04 (0.02)	0.05 (0.03)	0.08 (0.02)	NS

NS: non-significant. Mean (SD).

its corresponding bvFTD sample, and assessed following their institute's standard clinical examination.

Participants (or their Person Responsible) provided signed informed consent in accordance with the Declaration of Helsinki. The study protocol was approved by the institutional Ethics Committee of each center.

Image Acquisition

Structural imaging

Country-1 participants were scanned in a 1.5T Phillips Intera scanner with a standard head coil. We used a T1-weighted spin-echo sequence covering the whole brain (matrix size = 256 × 240 × 120, 1 mm isotropic; TR = 7,489 ms; TE = 3,420 ms; flip angle = 8°).

Country-2 participants underwent whole-brain structural T1-rapid gradient-echo (MP RAGE) scans in a 3T Philips Achieva (matrix size = 256 × 256 × 160, 1 mm isotropic; TR = 8,521 ms; TE = 4,130 ms; flip angle = 9°).

In Country-3, whole-brain structural T1-weighted spin echo sequences were acquired through a 3T Philips MRI scanner with standard head coil (matrix size = 256 × 200 × 256, 1 mm isotropic; TR = 5,903 ms: TE = 2,660 ms; flip angle = 8°).

Functional imaging

We obtained resting-state recordings with different scanners and acquisition parameters across centers (Table IB). They were instructed to keep their eyes closed, remain still, and avoid moving or thinking about anything in particular (Agosta et al., 2013; Farb et al., 2013; Garcia-Cordero et al., 2015; Seeley et al., 2009; Whitwell et al., 2011).

Structural Imaging Analysis

Voxel-based morphometry

A voxel-based morphometry (VBM) analysis with the Statistical Parametric Mapping software (SPM12) was performed to establish the global atrophy pattern in patients with neurodegeneration. As in previous research of our group (Baez et al., 2016a,b; Couto et al., 2013; Santamaria-Garcia et al., 2016), data were preprocessed on the DARTEL Toolbox following validated procedures (Ashburner and Friston, 2000). Prior to modulation, the images were segmented in gray matter, white matter, and cerebrospinal fluid volumes. Next, 12 mm full-width half-maximum kernel images were smoothed (Good et al., 2001) and normalized to MNI space.

Lesion mapping (FIS group)

Lesion masks were manually traced in native spaces according to visible damage on a T1 scan, then normalized to MNI space, and finally overlapped to obtain the lesion map.

Functional Imaging Preprocessing

FMRI preprocessing

The Data Processing Assistant for Resting-State fMRI (DPARSF) (Chao-Gan and Yu-Feng, 2010) was used for preprocessing as in previous studies (Garcia-Cordero et al., 2016; Melloni et al., 2016). Images were slice-time corrected, realigned, normalized and smoothed (Fig. 1A). We excluded participants showing head movements greater than 3 mm and/or rotations higher than 3°: five Country-1 patients (all with bvFTD) and four Country-3 patients (two with bvFTD and two with AD). No differences were found in the mean translational and mean rotational parameters among groups (Table IC).

Matrix construction

Using the Automated Anatomical Labeling (AAL)-Atlas (Tzourio-Mazoyer et al., 2002) –one of the most broadly used atlas in dementia network studies (Baggio et al., 2014; Li et al., 2013; Liu et al., 2012; Sanabria-Diaz et al., 2013; Sanz-Arigita et al., 2010; Seo et al., 2013a,b; Supekar et al., 2008; Xiang et al., 2013; Yao et al., 2010), and used in two previous fMRI studies on bvFTD with graph theory measures (Agosta et al., 2013; Sedeno et al., 2016)−, we extracted mean time-courses by averaging the BOLD signal of all voxels from each of the 90 regions of interest (ROIs). Pearson's correlation coefficient was used to construct a 90-node FC network for each subject (Fig. 1C). We discarded negative correlations, which are controversial and less systematic in resting-state (Rubinov and Sporns, 2010).

Functional Connectivity Analysis

We assessed FC with three methods: inter-regional connectivity, seed analysis, and graph-theory analysis.

Inter-regional connectivity

This analysis taps connectivity strength associations between each pair of regions (based on the 90-node functional connectivity network). It allows identifying altered pairwise connection patterns in bvFTD compared to controls. To this end, we used a network-based statistic (NBS) (Zalesky et al., 2010) to identify altered pairwise connections in bvFTD patients compared to controls (Fig. 1D). This is a nonparametric statistical method that controls the multiple comparisons problem and the family-wise error on a graph. Briefly, potentially connected structures (named, graph components) are derived from suprathreshold links, which are identified based on an "a priori" threshold applied to a two-sample *t*-test between controls and patients. To estimate the significant value of these components, their topological extension is compared against the null distribution of maximal connected component size that is calculated from a nonparametric permutation testing. The NBS yields greater

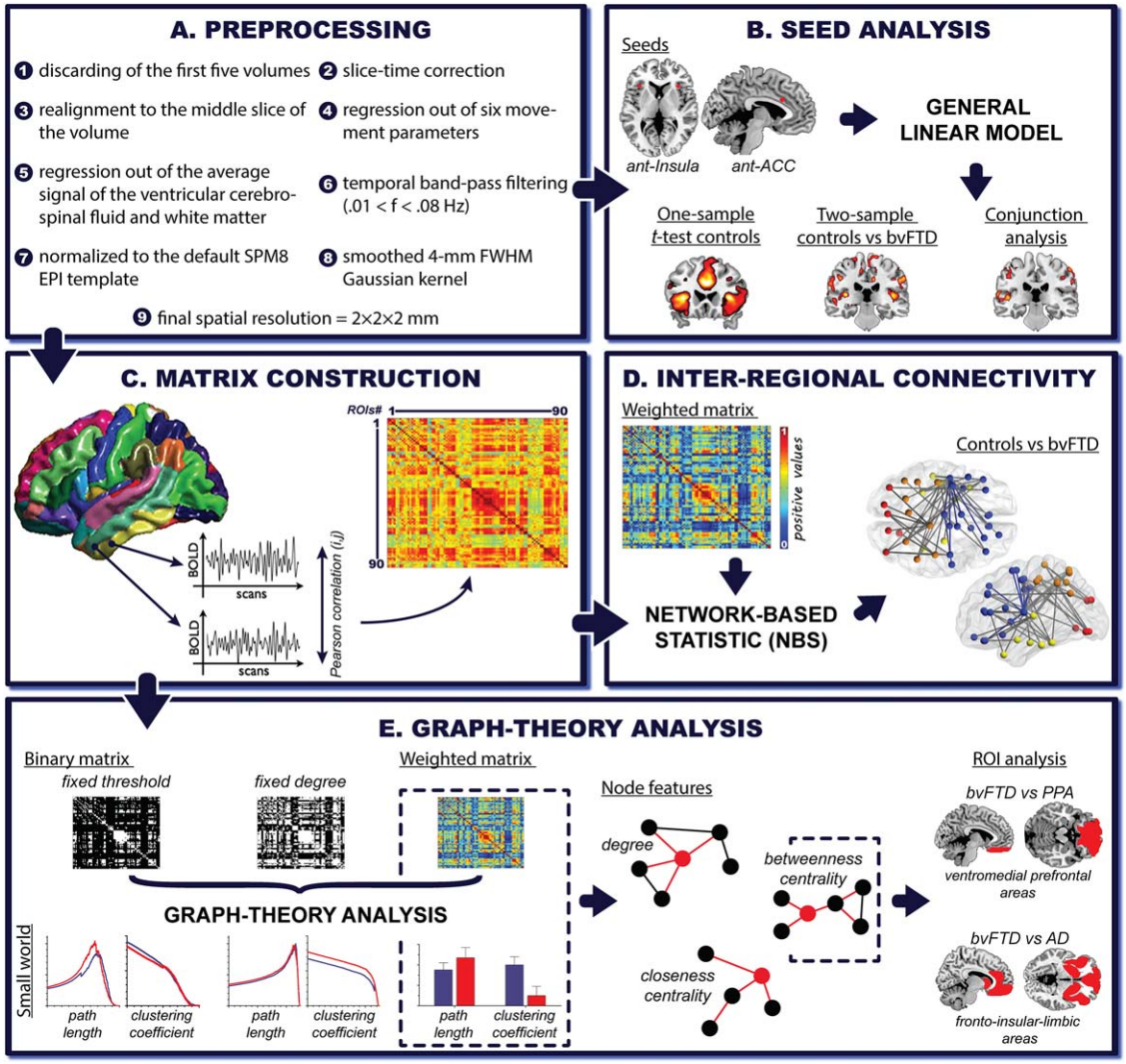

Figure 1.

fMRI: Preprocessing and analysis pipeline. A. Preprocessing: each fMRI preprocessing steps was performed using the DPARSF toolbox, an automated pipeline for resting-state fMRI data preprocessing previously used in graph-theory research (Cao et al., 2014) and in studies on FTD's functional connectivity features (Farb et al., 2013). B. Seed analysis: two bilateral seeds were selected, namely, the ACC (right $x = 5$; $y = 19$; $z = 28$ and left $x = -5$; $y = 19$; $z = 28$) and the anterior ventral insula (right $x = 35$; $y = 24$; $z = 5$; and left $x = -35$; $y = 24$; $z = 5$). Seeds consisted of 4-mm radius spheres. C. Matrix construction: Pearson's correlation coefficient was used to construct 90-node functional connectivity matrices per subject based on the Automated Anatomical Labeling (AAL)-Atlas. D. Inter-regional connectivity: NBS analyzes were performed over weighted undirected matrices (negative correlations were discarded), showing altered pairwise connections in bvFTD compared to controls. E. Graph-theory analysis: graph-theoretical measures were derived from binary (fixed threshold and fixed degree approaches) and weighted undirected matrices (negative correlations were discarded). For the fixed threshold approach, we analyzed 1,000 thresholds whose correlation values (*rho*) ranged from zero to one (*x* axis). In the fixed degree approach, the number of thresholds varied among countries to preserve a constant degree value across subjects (*x* axis, country one: 2,474 thresholds; country two: 2,453 thresholds and country three: 3,088 thresholds). We calculated the following measures: characteristic path length (L), that is, the average of the minimum number of edges that must be crossed to go from one node to any other node on the network and is taken as a measure of functional integration (Watts and Strogatz, 1998); average clustering coefficient (C), which indicates how strongly a network is locally interconnected and is considered a measure of segregation (Watts and Strogatz, 1998); degree (K), which represents the number of connections that link one node to the rest of the network (Bullmore and Sporns, 2009); closeness centrality (CC), namely, the inverse of the average shortest path length between one node and all the others in the network(Freeman, 1978); and betweenness centrality (BC), indicating the number of shortest paths that pass through a node and links the other node pairs across the network (Freeman, 1978). Finally, we compared bvFTD against PPA and AD based on a ROI analysis. These bilateral ROIs were selected according to previously reported atrophy differences between these diseases. The ventromedial prefrontal region involves one of the main areas specifically affected in bvFTD compared to PPA (Lu et al., 2013). The fronto-insular-limbic areas (inferior, medial, and superior orbitofrontal gyrus, gyrus rectus, insular cortex, ACC, putamen, pallidum and caudate) encompassed regions that are primarily affected in bvFTD when compared to AD (Irish et al., 2014; Rabinovici et al., 2007). [Color figure can be viewed at wileyonlinelibrary.com]

power than mass-univariate link analysis because the null hypothesis is rejected on a component-by-component level, overcoming the multiple comparison problem (Zalesky et al., 2010). In this way, results cannot be interpreted at the individual connection level but on a structural level. The NBS has already been used in neurodegenerative studies (Bai et al., 2012; Wang et al., 2013) [see technical details in (Zalesky et al., 2010)].

Seed analysis

We used seed analysis to explore differences between controls and patients—and similarities across countries—in the most important target network for bvFTD: the SN (Pievani et al., 2011, 2014). Two bilateral regions previously used in FTD studies to derive the SN were selected as seeds: ACC (Dopper et al., 2014) and the ventral anterior insula (Seeley et al., 2009) (see Fig. 1B). For each participant, BOLD signal time course from the voxels within each seed region were extracted and averaged together. Next, this averaged time series was correlated to every voxel in the brain using Pearson correlation coefficient. The whole-brain correlation maps from each seed were averaged together to finally derive the SN. The aim of this last step was to overcome possible disadvantages of estimating the intrinsic connectivity analysis from a single seed region (Demertzi et al., 2015).

Graph-theory analysis

Using the BCT toolbox (Bullmore and Sporns, 2009), we derived three approaches to graph-theoretical measures from binary and weighted undirected matrices (Rubinov and Sporns, 2010). To define the binary matrices, we applied two typical approaches (Stam et al., 2007; van den Heuvel et al., 2008) (Fig. 1E). The first procedure (fixed threshold approach) establishes an absolute value (that range from zero to one in 1,000 steps) to binarize the correlation coefficients between node-pairs. Values above/below this threshold are set to 1 and 0, respectively. The number of node-pairs that survive varies between subjects, so that networks from each participant may differ in size and degree (van Wijk et al., 2010). To avoid such differences, we applied a second procedure (fixed degree approach) in which the threshold is adjusted for each individual; hence the network size is fixed across subjects (van Wijk et al., 2010). Although this method overcomes network-size differences by forcing the same number of connections for all participants, it may modify network topology (van Wijk et al., 2010). Thus, small correlation values from networks with low average connectivity might surpass the threshold to achieve the fixed degree, while larger correlation values from networks with high average connectivity might not. Following state-of-the-art recommendations (Rubinov and Sporns, 2010), we explored multiple thresholds. Finally, to circumvent thresholding issues, we estimated graph measures from weighted undirected matrices while preserving information of each node-pair (van Wijk et al., 2010). However, weight differences across subjects might influence graph measures as in the fixed threshold approach (van Wijk et al., 2010).

Integration and segregation measures. We explored two extensively used measures to show efficient and ubiquitous small-world organization (Rubinov and Sporns, 2010) of the human brain (high levels of long-range integration combined with high levels of local connectivity): characteristic path length (L) and average clustering coefficient (C). These were analyzed to test possible group differences in the balance between efficient inter-nodal information transmission (low L values) and efficient local processing (high C values).

Nodal centrality features. These measures appraise the relevance of a node within a network (Rubinov and Sporns, 2010), for example by showing how many connections it has. We calculated the three most common nodal measures (Rubinov and Sporns, 2010) to characterize the centrality features of each region and the groups' global network centrality organization: (a) degree (K) –the total amount of connections of a node (Bullmore and Sporns, 2009)–; (b) closeness centrality (CC) –a node's overall integration with all the others in the network (Freeman, 1978)–; and (c) betweenness centrality (BC), –the centrality of a node's position in a network's information flow or integration (Freeman, 1978). These measures provide complementary information. K shows a node's involvement in a network regardless of its position. Thus, a highly connected node might possess abundant neighboring connections but very few long-range associations, indicating a peripheral role in the network's dynamics. On the other hand, CC and BC characterize the integration and relevance of a node, as they show whether it is closely connected to the others or represents a central path for inter-connections (Rubinov and Sporns, 2010).

Disease Control Groups

To test the specificity of our graph-theory results, we also assessed FIS, AD, and PPA patients. Given that only graph measures yielded robust results (see *Graph-theory analysis*), both global and nodal indexes from these groups were compared to those of bvFTD samples within their country.

Finally, we performed a ROI analysis to evaluate specific anatomical differences between bvFTD and the other two neurodegenerative diseases. ROIs were selected based on previous studies showing specific atrophy patterns of bvFTD patients compared to PPA (Lu, et al., 2013) and AD (Irish, et al., 2014; Rabinovici, et al., 2007) (Fig. 1E). For this assessment, we used one of the most sensitive graph indexes according to the above comparisons between bvFTD and controls.

Statistical Analysis

We used ANOVA and Pearson's chi-square tests within each country for demographic and movement comparisons.

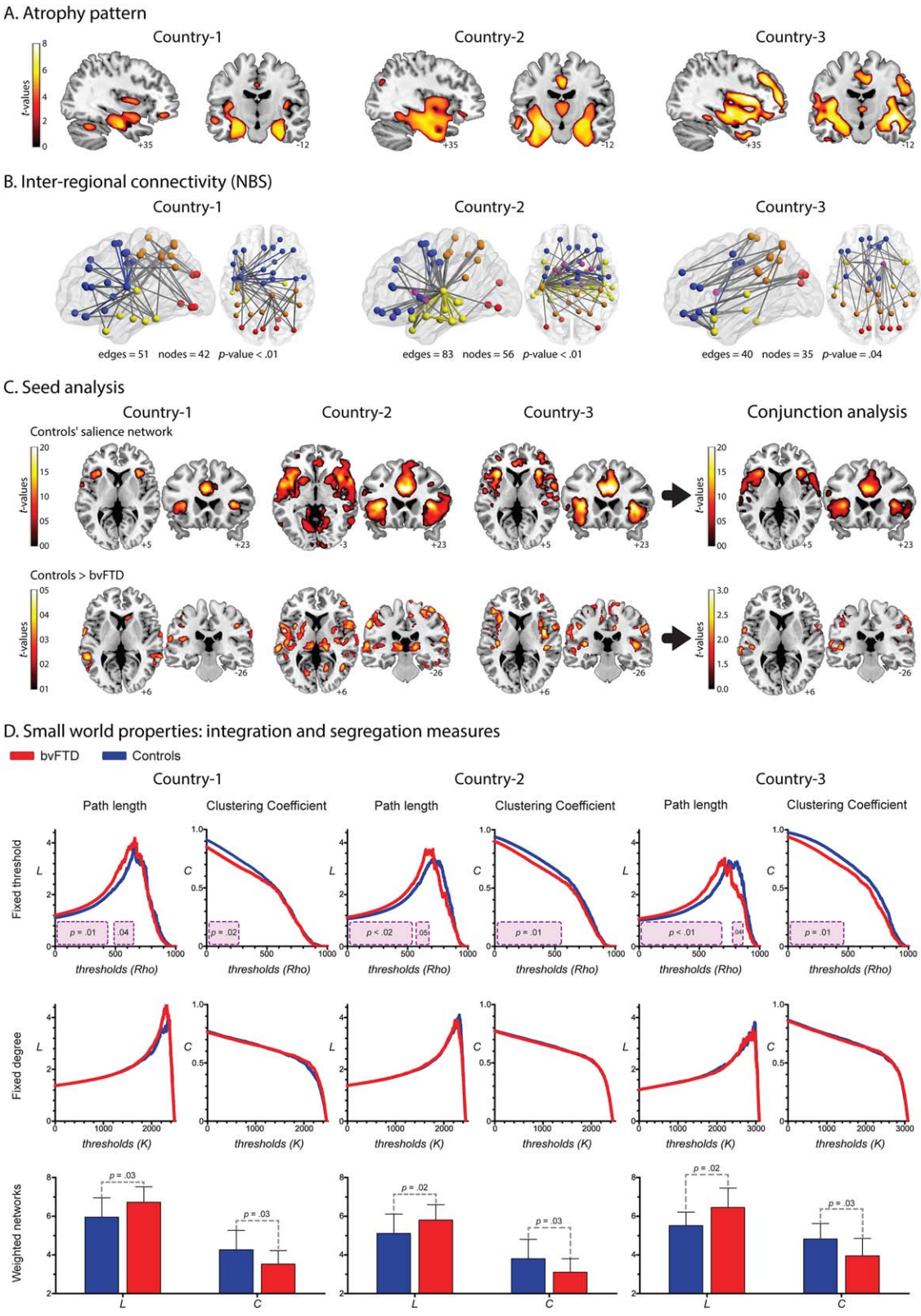
A. Atrophy pattern
Country-1
Country-2
Country-3
t-values
B. Inter-regional connectivity (NBS)
Country-1
Country-2
Country-3
edges = 51 nodes = 42 p-value < .01
edges = 83 nodes = 56 p-value < .01
edges = 40 nodes = 35 p-value = .04
C. Seed analysis
Country-1
Country-2
Country-3
Conjunction analysis
Controls' salience network
Controls > bvFTD
t-values
D. Small world properties: integration and segregation measures
bvFTD
Controls
Country-1
Country-2
Country-3
Path length
Clustering Coefficient
Fixed threshold
Fixed degree
Weighted networks
thresholds (Rho)
thresholds (K)
p = .01
p = .02
p = .03
p = .04
p = .05
L
C

Figure 2.

VBM (SPM12)

A two-sample *t*-test corrected by total intracranial volume was used to compare patients and controls across centers (FWE-corrected, $P = 0.05$, extent threshold = 100 voxels).

Inter-regional connectivity (NBS analysis)

Following state-of-the-art recommendations (Zalesky, et al., 2010), in our two-sample *t*-test between controls and patients we applied several a priori thresholds (ranging from *t*-value 3 to *t*-value 4) for each center. We used 5,000 permutations for this analysis (Fig. 1D).

Seed analysis (SPM12)

One-sample *t*-tests were applied to display connectivity maps in the control group of each center (FWE-corrected, $P = 0.05$, extent threshold = 50 voxels). The overlap of significant areas across centers was calculated through a conjunction analysis on the statistical maps of each one-sample *t*-test (FWE-corrected, $P = 0.05$, extent threshold = 50 voxels). Voxel-wise connectivity was compared between controls and bvFTD patients in the three countries with two-sample *t*-tests ($P = 0.001$ uncorrected, extent threshold = 50 voxels). A conjunction analysis was also performed to calculate the overlap of significant areas ($P = 0.05$ uncorrected, extent threshold = 50 voxels). These permissive thresholds were used to maximize the area of overlap of the differences between controls and patients across countries (Fig. 1B).

Graph measures (FieldTrip) (*Oostenveld et al., 2011*)

To compare controls against bvFTD patients from each center, we analyzed metrics derived from binary matrices with a specific cluster-based permutation tests (5,000 permutations) (Maris and Oostenveld, 2007). This analysis reduces the impact of comparing multiple thresholds in graph-theory (Sanz-Arigita et al., 2010; Sedeno et al., 2016), as it does not depend on multiple comparisons correction or assumptions about normal data distribution (Nichols and Holmes, 2002). It was implemented as in a previous report (Sedeno et al., 2016). Monte Carlo permutation tests (5,000 permutations) were combined with bootstrapping to assess global graph measures calculated from weighted matrices and ROI analyzes, as recommended (Bullmore and Bassett, 2011). Results from region level analysis are $P < 0.005$ uncorrected (Bai et al., 2012). Effect sizes were calculated with Cohen's *d* [in general interpreted as indicating small (0–0.20), medium (0.50–0.80) and large (>0.80) effects (Cohen, 1988)], which is recommend for measuring the magnitude of difference for independent sample *t*-test (Cohen, 1988) –that is the statistical method used in each permutation step.

RESULTS

Structural Imaging

Voxel-based morphometry

The atrophy pattern of bvFTD patients replicated previous results (Whitwell et al., 2009) and was consistent across countries (Fig. 2A) as shown by a conjunction analysis (see

Figure 2.

A. Atrophy pattern. VBM results (FWE-corrected, $P = 0.05$, extent threshold = 100 voxels) showed a consistent pattern of atrophy in the three countries (Whitwell et al., 2009), involving the main areas reported for bvFTD patients: ACC, the insular cortex, orbitofrontal areas, and medial temporal regions (hippocampus and amygdala). B. Inter-regional connectivity results. A single connected network, which involved different amounts of edges and nodes, was found altered in each country (*P*-value <0.01, corrected). Node color coding: frontal areas, blue; parietal regions, orange; temporal areas, yellow; limbic system, purple; occipital regions, red. Edge color: gray indicates altered connections between different regions and color highlights connections within a region. C. Seed analysis. The connectivity maps of the control samples across centers showed a very consistent engagement of the insular cortex and the ACC, two main areas related to the SN (FWE-corrected, $P = 0.05$, extent threshold = 50 voxels). Results from the comparison between controls and bvFTD are not consistent across countries ($P = 0.001$ uncorrected, extent threshold = 50 voxels). D. Graph results across countries: Integration and segregation measures. *Fixed-threshold* ($P < 0.05$, cluster-based corrected). Compared to controls, patients exhibited higher values of L. Country one: cluster one size from 0 *rho* to 0.41 *rho*; cluster two size from 0.48 *rho* to 0.62 *rho*; effect size 1.02. Country two: cluster one size from 0 *rho* to 0.5 *rho*; cluster two size from 0.60 *rho* to 0.66 *rho*; effect size 0.77. Country three: cluster one size from 0 *rho* to 0.66 *rho*; cluster two size from 0.76 *rho* to 0.83 *rho*; effect size 1.09. Regarding C, patients presented decreased values. Country one: cluster size from 0 *rho* to 0.26 *rho*; effect size 0.85. Country two: cluster size from 0 *rho* to 0.52 *rho*; effect size 0.75. Country three: cluster size from 0 *rho* to 0.45 *rho*; effect size 0.85. *Fixed-degree* ($P < 0.05$, cluster-based corrected). No differences were found in any of the countries. *Weighted undirected matrices* ($P < 0.05$). Patients exhibited higher values of L than controls. Country one: effect size 0.82. Country two: effect size 0.75. Country three: effect size 1.03. C was lower in patients than controls. Country one: effect size 0.80. Country two: effect size 0.73. Country three: effect size 0.94. [Color figure can be viewed at wileyonlinelibrary.com]

Supporting Information Fig. S1). Damage extended throughout the ACC, the insular cortex, orbitofrontal areas, and medial temporal regions (hippocampus and amygdala) (Ibanez and Manes, 2012) (Supporting Information Table S3).

Finally, to assess the reproducibility of atrophy patterns across countries, we performed a correlation analysis between the results of each dataset, following previously reported procedures. Correlation values higher than $Rho > 0.2$ were taken to indicate high consistency of results between pairs of datasets. Our VBM results showed large *Rho* values between countries: country-1 vs country-2, Rho = 0.77, P-value < 0.001; country-1 vs country-3, Rho = 0.85, P-value < 0.001; country-2 vs country-3, Rho = 0.75, P-value < 0.001 (see Supporting Information Fig. S2A).

Functional Connectivity

Inter-regional connectivity

In all centers, bvFTD showed decreased connectivity compared to controls (Fig. 2B), although compromised connection patterns were inconsistent across countries. Predominant left-sided alterations were observed in Country-1, whereas differences were concentrated in temporal and limbic-system connections in Country-2. In Country-3, differences were found predominantly in frontal-parietal connections. In addition, the final a priori threshold applied in these results was different for each center: while data from Country-1 and −2 were analyzed with the same threshold ($t = 4$), Country-3 only yielded significant results with a more permissive one ($t = 3.4$).

Seed analysis

We identified the main areas of the SN in controls: the insular cortex and the ACC (Fig. 2C). This was highly consistent across centers as shown by the conjunction analysis. However, the comparison between controls and bvFTD patients differed from country to country (Fig. 2C and Supporting Information Fig. S3). In Country-1, patients presented very few areas of decreased connectivity, mainly in the basal ganglia and frontal operculum. Reduced connectivity was also observed in Countries 2 and 3, mainly in insular regions; yet, this pattern was more posterior in Country-2 and more anterior in Country-3. Joint analysis of data from all centers confirmed that decreased connectivity in the SN was inconsistent across countries. Specifically, significant differences were found only with a very permissive threshold ($P < 0.05$, uncorrected) and the main SN areas (ACC, insula) were missing.

In addition, we assessed the consistency of these results using correlation analysis between datasets, as done on VBM findings. In this case, all the comparisons between pairs of countries yielded low correlation values ($Rho < 0.2$): country-1 vs country-2, Rho = −0.14; country-1 vs country-3, Rho = −0.09; country-2 vs country-3, Rho = −0.03 (see Supporting Information Fig. S2B).

Graph-theory analysis

Integration and segregation measures (Fig. 2D). Compared to controls, bvFTD patients presented significantly higher L in the three countries. This was observed only in the fixed threshold and weighted matrices approaches. The same was true of C, but here the patients exhibited significantly decreased values. Across countries, the magnitude of these differences was similar [effect sizes ranged from medium (0.75) to large (1.09)]. No differences were found in any measure with the fixed degree approach.

Nodal centrality features (Fig. 3). Since the weighted matrices analysis yielded the most consistent differences, only the node measures derived from this approach are reported. Although the fixed threshold method also revealed significant results, it presents the disadvantage of dealing with multiple thresholds. Global averages of node measures were consistent across countries: relative to controls, patients exhibited decreased K and CC, and increased BC. Figure 3A illustrates the consistency of nodal centrality alterations between countries. Lobes in which the bvFTD samples presented altered areas across datasets are highlighted in the figure through color circles. Results show that patients from the three countries showed common aberrant spatial organization in fronto-temporal areas (blue and yellow circles, respectively). In addition, Figure 3B offers a schematic representation in which four circles are presented for each brain lobe (fronto-limbic, temporal, parietal, and occipital lobes). For each measure and dataset, these circles were colored if bvFTD patients presented at least one aberrant centrality node within the lobe compared to controls. This figure shows that whereas several areas from different lobes were affected in patients, only the frontal-limbic regions were consistently compromised in the three countries and across measures (Supporting Information Table S4).

Finally, we merged the bvFTD (45) and control samples (60) of each country, and compared them using all global measures based on the weighted approach, and including scanning center as a confounding variable of the analysis. All the metrics yielded the same significant differences as when countries were separately analyzed (Supporting Information Table S5 for statistical details).

Disease Control Groups

The following analyzes rely on the weighted approach, which yielded the most robust and consistent graphmetric results across countries.

FIS

Frontal and insular structures were injured in the FIS group (as shown by Fig. 4 and Supporting Information Table S6). Global level analysis showed that bvFTD, relative to FIS, presented significantly decreased C, CC, and K as well as

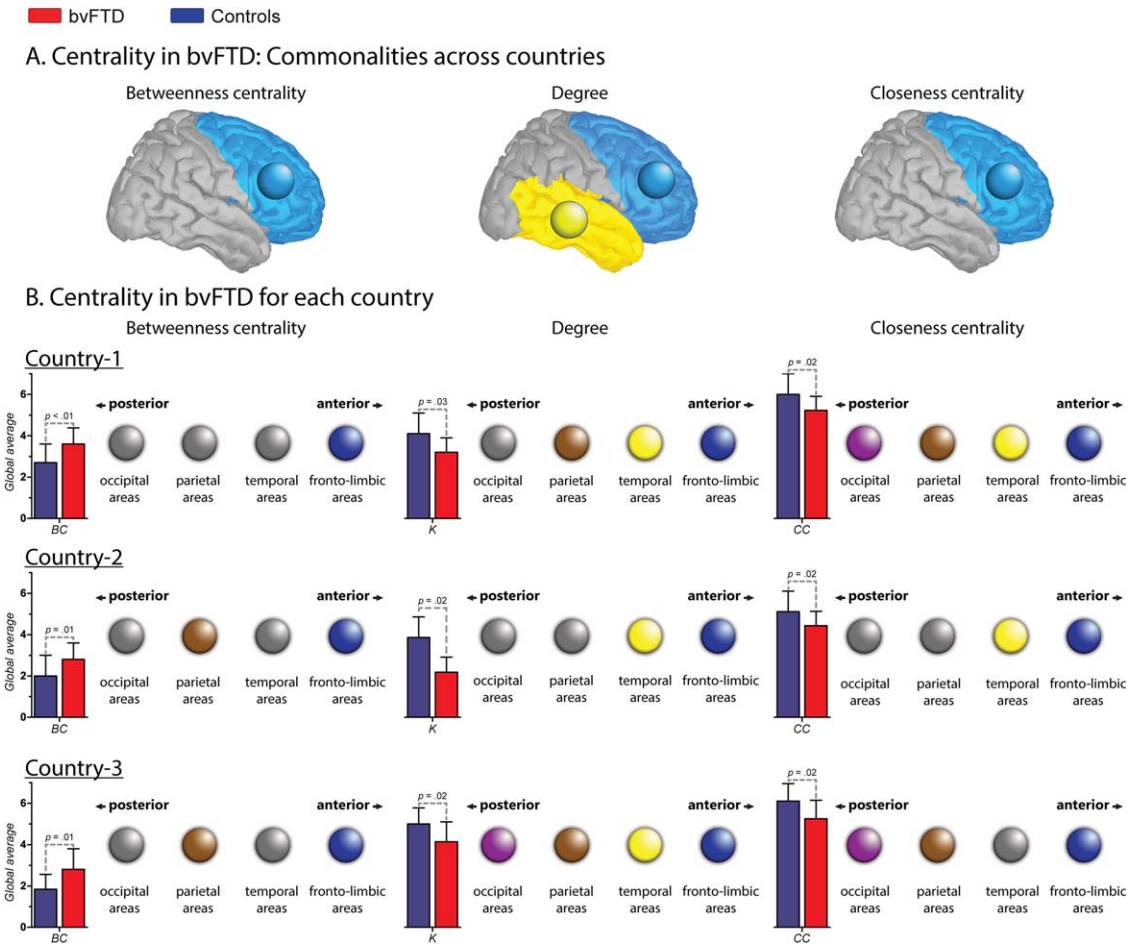

Figure 3.

Nodal centrality features. A. Centrality in bvFTD: Communalities across countries. Circles indicate brain lobes in which the bvFTD patients presented altered areas within the same lobe across countries. In BC and CC, the common areas affected belong to the fronto-limbic lobe, while in K, they belong both to the fronto-limbic and temporal lobes. B. Centrality in bvFTD for each country. Color circles indicate the presence of at least one altered region within the specific lobe (pink = occipital; brown = parietal; yellow = temporal and blue = fronto-limbic). Gray circles represent the absence of alterations within the lobe. Bar charts represent the global average (GA) of each centrality measure. *Country one*. Effect size of the GA of BC: 1.00. Regions with increased BC in patients: right putamen and right middle orbitofrontal cortex (fronto-limbic areas). Effect size of the GA K: 0.91. Regions with decreased K in patients: right precentral gyrus, left rolandic operculum, right and left fusiform gyrus, right postcentral gyrus and left superior parietal cortex. Effect size of the GA CC: 0.84. Regions with decreased CC in patients: right precentral gyrus, left rolandic operculum, right and left fusiform, right postcentral gyrus, and right and left occipital inferior lobe. *Country two*. Effect size of the GA of BC: 0.77. Regions with increased BC in patients: left precentral gyrus, right insular cortex, right posterior cingulate cortex, right supramarginal gyrus and left angular gyrus. Effect size of the GA K: 0.75. Regions with decreased K in patients: right and left amygdala, right and left heschl's gyrus, right superior temporal pole and right middle temporal pole. Effect size of the GA CC: 0.75. Regions with decreased CC in patients: right superior frontal gyrus, left middle cingulate cortex, right and left Heschl's gyrus, right superior temporal pole, right and left middle temporal pole and right inferior temporal gyrus. *Country three*. Effect size of the GA of BC: 1.05. Regions with increased BC in patients: left Rolandic operculum, left medial orbitofrontal cortex, right angular gyrus and left precuneus. Effect size of the GA K: 1.00. Regions with decreased K in patients: right and left superior orbitofrontal cortex, right middle temporal pole, right paracentral lobe, right calcarine sulcus, right cuneus and lingual gyrus. Effect size of the GA CC: 0.92. Regions with decreased CC in patients: right and left superior orbitofrontal cortex, right paracentral lobe, right calcarine sulcus, and right cuneus gyrus. [Color figure can be viewed at wileyonlinelibrary.com]

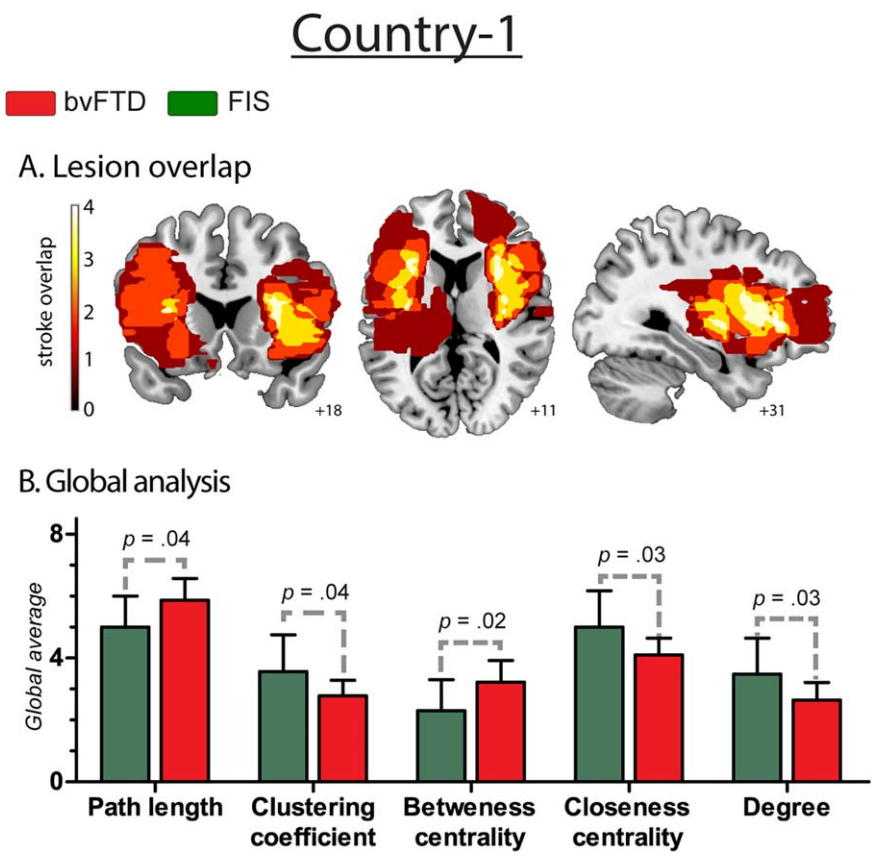

Figure 4.

Results regarding fronto-insular stroke patients. A. Lesion overlap. Frontal and insular structures that were injured in stroke patients. The colormap indicates lesions overlapping across the group: dark red refers to areas affected by the lesion of only one subject, while white shows injured areas shared by four patients. B. Global analysis. Effect size of global measures. L: 0.85; C: 0.85; BC: 0.93; CC: 0.95, and K: 0.93. [Color figure can be viewed at wileyonlinelibrary.com]

significantly higher values in L and BC (see Supporting Information Table S7 for further details of FIS graph-theory measures).

PPA

PPA patients presented fronto-temporal atrophy with left-side predominance (Agosta et al., 2012) (Fig. 5A and Supporting Information Table S3). Relative to controls, they showed alterations in global and average nodal measures, resembling those found in bvFTD (Fig. 5B). Node-level comparisons between controls and PPA patients revealed widespread differences in BC, K, and CC across parietal, temporal, and fronto-limbic areas (Fig. 5C and Supporting Information Table S4). These results replicate those obtained in the comparison between bvFTD patients and controls. This was expected given that both forms of dementia involve similar atrophy patterns affecting mainly fronto-insulo-temporal areas (Figs. 2 and 5).

Specific differences between these two diseases were nevertheless present in terms of BC –the only nodal measure investigated given its large effect size in the comparison between controls and patients in all countries. First, across graph measures, the average BC was significantly higher in PPA than in bvFTD patients (Fig. 5B). Second, ROI analysis of BC in the ventromedial prefrontal region, an area specifically compromised in bvFTD compared to PPA (Lu et al., 2013), revealed significantly higher BC in the latter in the left side of this region (Fig. 7).

AD

AD patients showed an expected (Du et al., 2007) volume loss mainly comprising temporoparietal regions (Fig. 6A and Supporting Information Table S3). Global and average nodal alterations in AD relative to controls were similar to those found in bvFTD (Fig. 6B). These overall patterns replicate previous findings in both diseases (Agosta et al., 2013; Pievani et al., 2011). Also, node-level comparisons between AD and controls yielded consistent differences in posterior (occipital and parietal regions) and

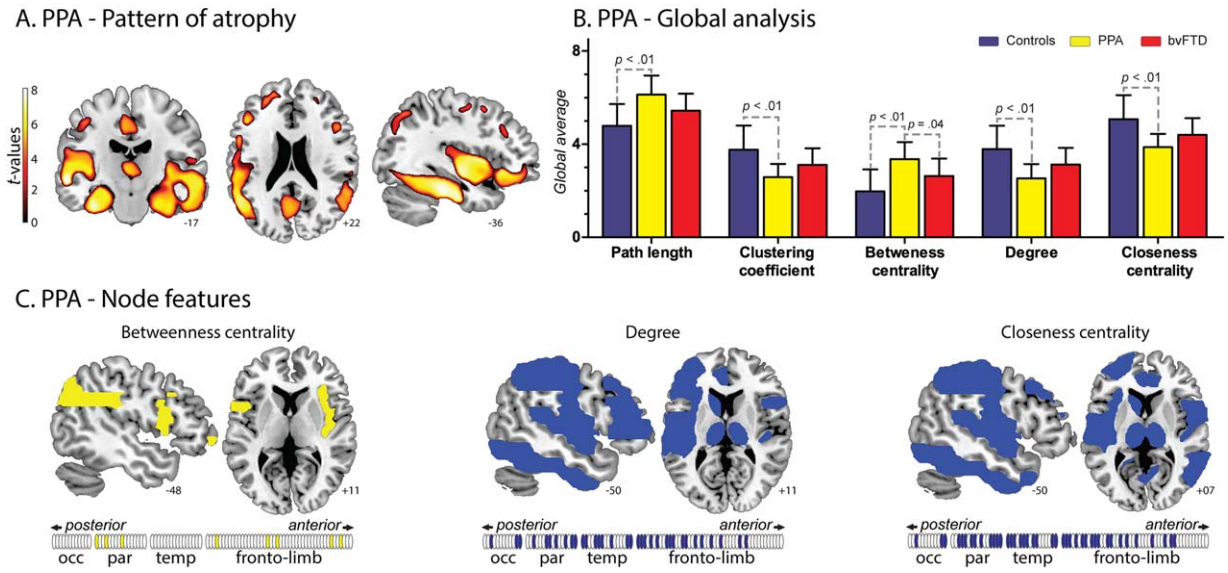

Figure 5.

Results regarding PPA patients from Country-2. A. Atrophy pattern. VBM results showed a fronto-temporal pattern of atrophy with left-side predominance. B. Global analysis. Effect sizes of the significant differences between PPA and controls. L: 1.46; CC: 1.42; BC: 1.58; CC: 1.46 and K: 1.49. Effect sizes of the significant differences between PPA and bvFTD. BC: 0.92. C. Nodal centrality features. Compared to controls, PPA patients presented decreased values of K and CC in a distributed manner affecting parietal, temporal and fronto-limbic areas, and an increased value of BC in parietal and fronto-limbic areas. [Color figure can be viewed at wileyonlinelibrary.com]

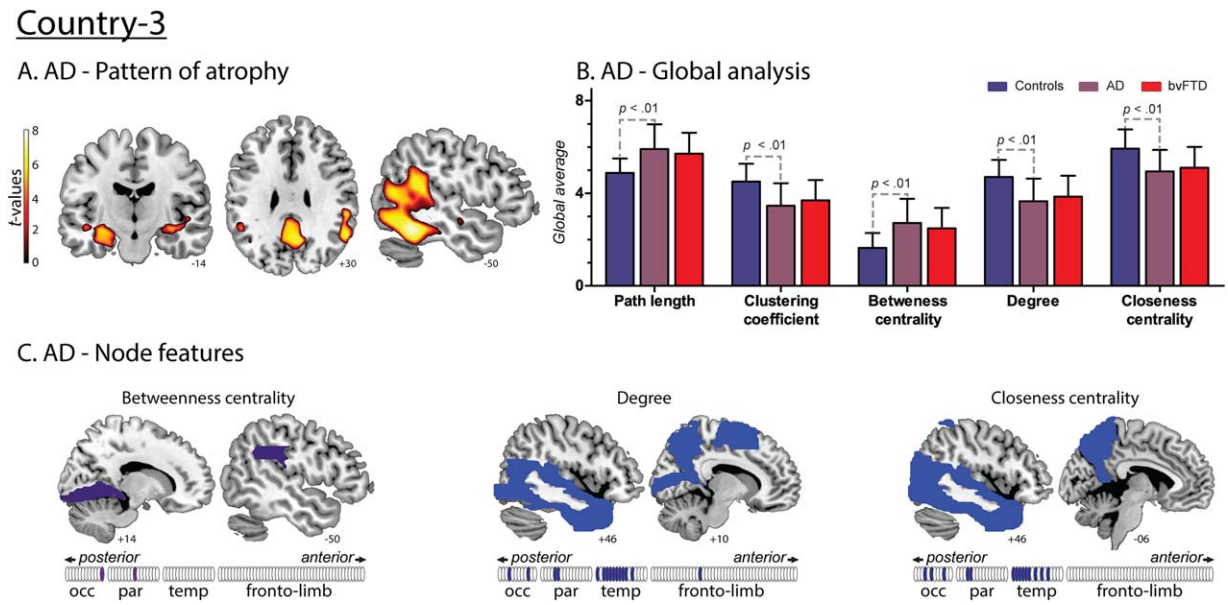

Figure 6.

Results regarding AD patients from Country-3. A. Atrophy pattern. VBM results presented atrophy mainly in the hippocampus and parahippocampus, precuneus, posterior cingulate cortex and posterior temporal regions. B. Global analysis. Effect sizes of the significant differences between AD and controls. L: 1.17; C: 1.15; BC: 1.22; CC: 1.08 and K: 1.18. No differences were found between AD and bvFTD. C. Nodal centrality features. Compared to controls, AD patients presented decreased values of K and CC in temporal, parietal and occipital regions and an increased value of BC in parietal and occipital areas. [Color figure can be viewed at wileyonlinelibrary.com]

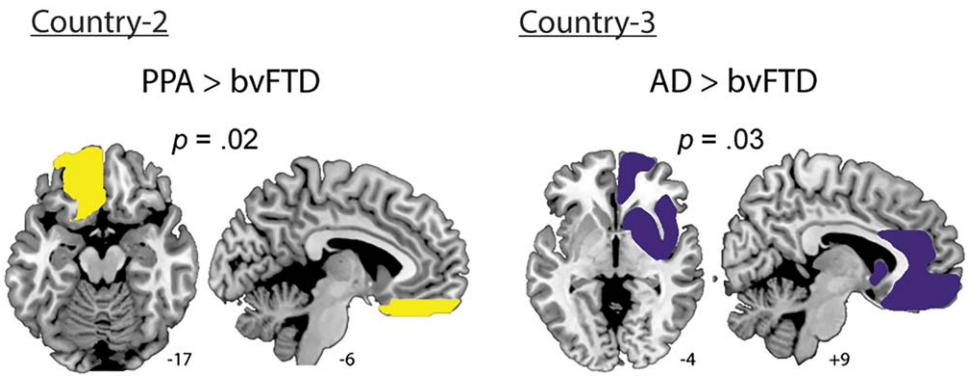

Figure 7.
ROI analysis. A. Country two: PPA patients presented a higher BC than the bvFTD group in the ventromedial prefrontal region (effect size: 1.04). B. Country three: AD showed a higher BC than bvFTD in the right fronto-limbic ROI (effect size: 0.90). [Color figure can be viewed at wileyonlinelibrary.com]

temporal areas, across all graph indexes (Fig. 6C and Supporting Information Table S4). In contrast to bvFTD, AD featured no disturbance of frontal network centrality. This differential pattern represents a first step to establish network alterations specific to each disease, despite the presence of similar global changes.

Finally, to corroborate this specific alteration of frontal networks in bvFTD, we analyzed a ROI encompassing fronto-insular limbic areas, which are primarily atrophied in bvFTD relative to AD (Irish et al., 2014; Rabinovici et al., 2007). As was the case with PPA patients, our analysis focused on BC: AD patients presented higher values than bvFTD in the right fronto-limbic ROI. This result aligned with those obtained in the nodal comparison, and supported the specificity of frontal alterations in bvFTD (Fig. 7).

DISCUSSION

In this unprecedented connectivity multicenter report in bvFTD, we assessed the sensitivity and specificity of FC methods to detect connectivity abnormalities in this disease. Graph-theory was the only method which consistently discriminated bvFTD patients from controls and other neurological samples across centers. Thus, graph-theory might become a gold-standard approach for brain network analysis, irrespective of methodological, diagnostic, and sociocultural factors. Our findings might represent an important step to identify clinically relevant neuromarkers of neurodegenerative diseases.

Sensitivity of Graph-Theory Metrics in bvFTD

Graph-theory metrics robustly discriminated bvFTD patients from controls across centers. In particular, small-world measures revealed alterations in the integration of distant regions (L) and in local processing (C). Such disturbed balance between integration and segregation suggests inefficient information transfer between both regionally and distributed brain areas.

Also, global measures of node centrality showed decreased connectivity (K) and nodal integration (CC) in bvFTD. However, such results were more diverse at node level across countries, confirming that graph measures are less reliable when considering this unit (Telesford et al., 2013). Yet, temporal and frontal regions consistently presented less interconnected and integrated nodes in all patients. Given that both regions are anatomical hallmarks of bvFTD (Whitwell et al., 2009), node centrality measures seem capable of tapping its distinctive pathophysiology.

Notably, results regarding the central position of each node (BC) revealed an opposite pattern. At the global and nodal levels, nodes from bvFTD occupied a more central path between network connections. At first glance, this pattern of high central position nodes seems at odds with previous measures revealing a severely disconnected network. However, available evidence illuminates the issue. First, Agosta et al. (2013) reported that bvFTD patients showed a trend toward higher values of BC in parietal and frontal regions. Second, a heterogeneous pattern of increased and decreased BC has also been found in AD (Tijms et al., 2013). Such seemingly disparate findings might be reflecting the so-called overload breakdown problem (Holme, 2002): when a node loses connections, its load is redistributed to other nodes, which thus increase their participation in the network (Holme, 2002). In our study, nodes of bvFTD patients exhibited generalized loss of connections (as shown by the other graph measures). Ensuing network reorganization could have increased the central position of other nodes. While an in-depth assessment of the overload breakdown problem is beyond the scope of our paper, it may afford a useful framework to analyze network evolution in dementia.

In sum, consistent results across countries further support the relevance of BC as a marker of network abnormalities in bvFTD. Compared to the other measures, it revealed the highest differences between groups (based on effect sizes) at both global and nodal levels. Moreover, as discussed below, it also discriminated among different forms of dementia and stroke.

Specificity of Graph-Theory Metrics in bvFTD

Graph measures also revealed differences between bvFTD and other neurological conditions. Specifically, bvFTD differed from FIS in global connectivity patterns, while its differences relative to other neurodegenerative diseases mainly concerned node-level patterns.

As compared to FIS, bvFTD exhibited decreased integration of long-range connections and local connectivity, together with increased node centrality. Although similar brain structures were affected in both conditions, differential network compromise was expected given their etiological and pathophysiological specificities. Strokes involve focal tissue loss followed by neural reorganization and plasticity (Garcia-Cordero et al., 2015); when recovery is good, normal connectivity is restored in the months after the stroke (Grefkes and Fink, 2014). Conversely, neurodegeneration in bvFTD and AD implies diffuse damage mainly triggered by insidious protein aggregation. Thus, while focal damage in FIS would alter specific connections without affecting whole-brain dynamics, the pathological processes of dementia may disturb general network properties.

A different pattern of contrasts emerged upon comparing bvFTD with PPA and AD, all of which share gross neurodegenerative processes. Aberrant network organization has been reported in bvFTD (Agosta et al., 2013; Sedeno et al., 2016), AD (Pievani et al., 2011), and variants of PPA (Agosta et al., 2014). Predictably, no global-level differences emerged between groups. This was true for AD and for almost all measures in PPA. The latter condition featured significantly higher BC than bvFTD, suggesting more severe neurodegeneration. Two findings support this idea: first, though not statistically significant, means of all global measures pointed to a more disconnected network in PPA; second, at node level, more regions were affected in PPA than bvFTD (Supporting Information Table S4). The more disconnected network in PPA suggests that more nodes lost connections, which, as argued above, may overload other nodes. If the average network we are comparing is indeed more disconnected in PPA than bvFTD, then nodes in the former condition could have become reorganized toward more central positions.

Conversely, node-level and ROI analyzes showed different patterns between diseases. In comparing bvFTD and PPA, clear differences emerged only upon analyzing the ventromedial prefrontal region (an area that is specifically affected in the former condition compared to PPA). This suggests that the loss of connections in both diseases generated different patterns of centrality re-distribution. Frontal areas in bvFTD presented a peripheral role in the network's dynamics, in line with their characteristic atrophy pattern. On the other hand, PPA preserved the central role of these regions –which are not specific targets of this disease– despite their general loss of connectivity. In AD, the contrast with bvFTD was stronger. This was expected, since the atrophy pattern of bvFTD is more similar to that of PPA than that of AD. First, at node level, AD compared to controls showed alteration in posterior regions without almost any involvement of frontal hubs. This pattern opposes the one obtained in bvFTD, where the most consistent differences across countries were in frontal areas. Furthermore, as observed for PPA, when bvFTD were compared to AD, ROI results showed affected BC of bvFTD target areas (fronto-limbic regions) (Irish et al., 2014; Rabinovici et al., 2007).

In sum, previously proposed features of aberrant network organization in bvFTD (Agosta et al., 2013) were systematically detected across heterogeneous contexts. Furthermore, we showed that graph-theory discriminated bvFTD from FIS and, more interestingly, from other neurodegenerative conditions. Thus, graph measures might reveal potential biomarkers of bvFTD, paving the way for innovations in early diagnosis and monitoring of disease progression, therapeutic interventions, and other forms of clinical response.

Methodological Issues

We compared three methods based on FC: inter-regional connectivity, seed analysis, and graph-theory analysis. Crucially, only the latter yielded consistent results across countries.

Inter-regional connectivity and seed analysis corroborated connectivity alterations in bvFTD (Pievani et al., 2011, 2014). However, both analyzes, focused on voxel- or node-level connection patterns, failed to show consistent patterns across samples. For example, the conjunction assessment of the seed-analysis showed a minimum overlap of SN alterations between countries, and this inconsistency was further supported by the low correlation values between the results of each pair of datasets (see Supporting Information Fig. S2B). Note that the number of elements included by this method is above the thousands, which increases the degrees of freedom and, hence, the potential variability of results. A similar situation occurred with interregional connectivity analysis: different patterns of decreased connectivity were found across datasets. Compared to the seed-analysis, this measure was more inconsistent given that alterations were found with different statistical thresholds, indicating that strength differences were not persistent across countries. This could reflect reduced voxel-wise information due to the use of ROIs. Also, this method only captures the interaction between pairs of ROIs and it is not able to account for the complex interactions between areas that underpin the

organization and dynamics of the brain network (Telesford et al., 2011).

Also, though based on fewer, simpler measures, graph-theory analyzes corroborated this alteration with even greater consistency. This was true for two of the three approaches: fixed threshold and weighted matrices. Indeed, the fixed degree approach failed to identify expected differences (Agosta et al., 2013) between bvFTD and controls across countries. In this analysis, the threshold for binarizing subjects' connectivity matrix is adjusted to fix a similar network size across the whole sample (Fornito et al., 2013; Garrison et al., 2015; van den Heuvel et al., 2008; van Wijk et al., 2010). This might emphasize small correlation values from networks with low average connectivity networks, while over-underrating large correlations from network with higher connectivity (Fornito et al., 2013; Garrison et al., 2015; van den Heuvel et al., 2008; van Wijk et al., 2010). Thus, this approach might over-estimate the low connectivity values of bvFTD patients (as shown by the inter-regional and seeds analysis methods) and fail to capture their connectivity alterations. Conversely, the fixed threshold approach yielded consistent differences across countries. Application of the same threshold for all subjects avoids the over or underestimation of connectivity values, thus acknowledging hypoconnectivity patterns in the patients. These results replicate previous network alterations found in bvFTD through the same approach (Agosta et al., 2013). Despite this consistency, this method has its own limitations given that the fixed threshold generates networks of different size or degree that might bias the comparisons between groups (Fornito et al., 2013; Garrison et al., 2015; van den Heuvel et al., 2008; van Wijk et al., 2010). Accordingly, several studies have employed the fixed degree approach and showed network alterations in other dementias, such as AD (Brier et al., 2014; Liu et al., 2012; Xiang et al., 2013) and Parkinson's disease (Baggio et al., 2014). In sum, both network analyzes based on binary matrices present methodological constrains that might hinder their application as standard approaches to evaluate graph-theory measures.

On the other hand, the weighted approach overcomes these limitations and proves particularly interesting as it avoids dealing with multiple thresholds. In network analysis, no consensus exists on which thresholding level to apply or how many thresholds to consider (Bullmore and Sporns, 2009). Conveniently, the weighted approach circumvents these issues, preserves the information of each node (van Wijk et al., 2010), and facilitates between-group comparisons as it considers only one value to analyze a specific network phenomenon. Thus, it can simplify monitoring of disease progression, clinical response to interventions, and characterization of individual impairments. In sum, our findings indicate that interregional connectivity might be the less reliable method across countries, and that, in line with previous recommendations (Fornito et al., 2013; Reijneveld et al., 2007), the weighted graph measure might be a potential gold-standard approach for brain network analysis.

Limitations and Future Studies

Although each group's size was moderate, similar (and smaller) sizes have been used in recent FC studies (Farb et al., 2013). Moreover, the consistency of our findings suggests that they were not biased by the number of subjects. Also, there are other graph measures that might provide valuable information about brain network alterations in dementia (such as modularity, global efficiency, etc.); however, their analysis was beyond our scope given the amount of results presented, and that we assessed relevant graph measure as the small-world and centrality index. Brain parcellation is another methodological constrain given its effect in FC and graph-theory (Fornito et al., 2010). Future studies should evaluate the replicability of our findings with different parcellation resolutions, and preserving regions sizes. Finally, we were unable to apply graph-theory in genetic forms of bvFTD during presymptomatic stages, monitoring disease progression and network reconfiguration following clinical therapy; it would be crucial to extend our report through longitudinal studies.

CONCLUSIONS

FTD is the second most common dementia in patients below age 65 (Piguet et al., 2011a). Its relatively young onset, its clinical overlap with other diseases, and its variable pattern of brain atrophy make it difficult to achieve early diagnosis via conventional neuropsychological assessments or routine clinical neuroimaging (Ibanez et al., 2014, 2016, Piguet et al., 2011a). Accurate early diagnosis is fundamental to foster timely therapeutic intervention, study potential disease-modifying agents, and alleviate associated financial burdens (Prince et al., 2015). Graph-theory might become an important tool to achieve these aims. In this unprecedented multicenter study, we took a first step in this direction by showing that graph-theory metrics reveal condition-specific FC alteration in bvFTD, which are robust enough to emerge despite major variability across countries. Further research is needed to confirm the reliability of these results; however, the consistency of our findings supports graph-theory as a potential gold-standard for brain network analyzes, and highlights its eventual role as a biomarker signature for dementias.

REFERENCES

Agosta F, Canu E, Sarro L, Comi G, Filippi M (2012): Neuroimaging findings in frontotemporal lobar degeneration spectrum of disorders. Cortex 48:389–413.

Agosta F, Galantucci S, Valsasina P, Canu E, Meani A, Marcone A, Magnani G, Falini A, Comi G, Filippi M (2014): Disrupted brain connectome in semantic variant of primary progressive aphasia. Neurobiol Aging 35:2646–2655.

Agosta F, Sala S, Valsasina P, Meani A, Canu E, Magnani G, Cappa SF, Scola E, Quatto P, Horsfield MA, Falini A, Comi G, Filippi M (2013): Brain network connectivity assessed using

graph theory in frontotemporal dementia. Neurology 81: 134–143.
Ashburner J, Friston KJ (2000): Voxel-based morphometry–the methods. NeuroImage 11:805–821.
Baez S, Couto B, Torralva T, Sposato LA, Huepe D, Montanes P, Reyes P, Matallana D, Vigliecca NS, Slachevsky A, Manes F, Ibanez A (2014): Comparing moral judgments of patients with frontotemporal dementia and frontal stroke. JAMA Neurol 71: 1172–1176.
Baez S, Kanske P, Matallana D, Montanes P, Reyes P, Slachevsky A, Matus C, Vigliecca NS, Torralva T, Manes F, Ibanez A (2016a): Integration of intention and outcome for moral judgment in frontotemporal dementia: Brain structural signatures. Neurodegener Dis 16:206–217.
Baez S, Morales JP, Slachevsky A, Torralva T, Matus C, Manes F, Ibanez A (2016b): Orbitofrontal and limbic signatures of empathic concern and intentional harm in the behavioral variant frontotemporal dementia. Cortex 75:20–32.
Baggio HC, Sala-Llonch R, Segura B, Marti MJ, Valldeoriola F, Compta Y, Tolosa E, Junque C (2014): Functional brain networks and cognitive deficits in Parkinson's disease. Hum Brain Mapp 35:4620–4634.
Bai F, Shu N, Yuan Y, Shi Y, Yu H, Wu D, Wang J, Xia M, He Y, Zhang Z (2012): Topologically convergent and divergent structural connectivity patterns between patients with remitted geriatric depression and amnestic mild cognitive impairment. J Neurosci 32:4307–4318.
Brier MR, Thomas JB, Fagan AM, Hassenstab J, Holtzman DM, Benzinger TL, Morris JC, Ances BM (2014): Functional connectivity and graph theory in preclinical Alzheimer's disease. Neurobiol Aging 35:757–768.
Bullmore E, Sporns O (2009): Complex brain networks: graph theoretical analysis of structural and functional systems. Nat Rev Neurosci 10:186–198.
Bullmore ET, Bassett DS (2011): Brain graphs: graphical models of the human brain connectome. Annu Rev Clin Psychol 7:113–140.
Cao H, Plichta MM, Schafer A, Haddad L, Grimm O, Schneider M, Esslinger C, Kirsch P, Meyer-Lindenberg A, Tost H (2014): Test-retest reliability of fMRI-based graph theoretical properties during working memory, emotion processing, and resting state. NeuroImage 84:888–900.
Cohen, J. (1988) Statistical power analysis for the behavioral sciences. Hillsdale, N.J: L. Erlbaum Associates.
Couto B, Manes F, Montanes P, Matallana D, Reyes P, Velasquez M, Yoris A, Baez S, Ibanez A (2013): Structural neuroimaging of social cognition in progressive non-fluent aphasia and behavioral variant of frontotemporal dementia. Front Hum Neurosci 7:467.
Chao-Gan Y, Yu-Feng Z (2010): DPARSF: A MATLAB Toolbox for "Pipeline" data analysis of resting-state fMRI. Front Syst Neurosci 4:13.
De Vico Fallani F, Richiardi J, Chavez M, Achard S (2014): Graph analysis of functional brain networks: practical issues in translational neuroscience. Philos Trans R Soc Lond B Biol Sci 369. doi:10.1098/rstb.2013.0521.
Demertzi A, Antonopoulos G, Heine L, Voss HU, Crone JS, de Los Angeles C, Bahri MA, Di Perri C, Vanhaudenhuyse A, Charland-Verville V, Kronbichler M, Trinka E, Phillips C, Gomez F, Tshibanda L, Soddu A, Schiff ND, Whitfield-Gabrieli S, Laureys S (2015): Intrinsic functional connectivity differentiates minimally conscious from unresponsive patients. Brain 138:2619–2631.
Dopper EG, Rombouts SA, Jiskoot LC, den Heijer T, de Graaf JR, de Koning I, Hammerschlag AR, Seelaar H, Seeley WW, Veer IM, van Buchem MA, Rizzu P, van Swieten JC (2014): Structural and functional brain connectivity in presymptomatic familial frontotemporal dementia. Neurology 83:e19–e26.
Du AT, Schuff N, Kramer JH, Rosen HJ, Gorno-Tempini ML, Rankin K, Miller BL, Weiner MW (2007): Different regional patterns of cortical thinning in Alzheimer's disease and frontotemporal dementia. Brain 130:1159–1166.
Farb NA, Grady CL, Strother S, Tang-Wai DF, Masellis M, Black S, Freedman M, Pollock BG, Campbell KL, Hasher L, Chow TW (2013): Abnormal network connectivity in frontotemporal dementia: evidence for prefrontal isolation. Cortex 49: 1856–1873.
Fornito A, Zalesky A, Breakspear M (2013): Graph analysis of the human connectome: promise, progress, and pitfalls. NeuroImage 80:426–444.
Fornito A, Zalesky A, Bullmore ET (2010): Network scaling effects in graph analytic studies of human resting-state FMRI data. Front Syst Neurosci 4:22.
Freeman L (1978): Centrality in social networks conceptual clarification. Soc Network 1:215–239.
Garcia-Cordero, I., Sedeno, L., De la Fuente, L.A., Slachevsky, A., Forno, G., Klein, F., Lillo, P., Ferrari, J., Rodriguez, C., Bustin, J., Torralva, T., Baez, S., Yoris, A., Esteves, S., Melloni, M., Salamone, P., Huepe, D., Manes, F., Garcia, A.M., Ibanez, A. (2016) Feeling, learning from and being aware of inner states: interoceptive dimensions in neurodegeneration and stroke. Philos Trans R Soc B. 371:20160006. doi:10.1098/rstb.2016.0006.
Garcia-Cordero I, Sedeno L, Fraiman D, Craiem D, de la Fuente LA, Salamone P, Serrano C, Sposato L, Manes F, Ibanez A (2015): Stroke and neurodegeneration induce different connectivity aberrations in the insula. Stroke 46:2673–2677.
Garrison KA, Scheinost D, Finn ES, Shen X, Constable RT (2015): The (in)stability of functional brain network measures across thresholds. NeuroImage 118:651–661.
Good CD, Johnsrude IS, Ashburner J, Henson RN, Friston KJ, Frackowiak RS (2001): A voxel-based morphometric study of ageing in 465 normal adult human brains. NeuroImage 14: 21–36.
Gorno-Tempini ML, Hillis AE, Weintraub S, Kertesz A, Mendez M, Cappa SF, Ogar JM, Rohrer JD, Black S, Boeve BF, Manes F, Dronkers NF, Vandenberghe R, Rascovsky K, Patterson K, Miller BL, Knopman DS, Hodges JR, Mesulam MM, Grossman M (2011): Classification of primary progressive aphasia and its variants. Neurology 76:1006–1014.
Grefkes C, Fink GR (2014): Connectivity-based approaches in stroke and recovery of function. Lancet Neurol 13:206–216.
Henley SM, Bates GP, Tabrizi SJ (2005): Biomarkers for neurodegenerative diseases. Curr Opin Neurol 18:698–705.
Holme P (2002): Edge overload breakdown in evolving networks. Phys Rev E Stat Nonlin Soft Matter Phys 66:036119.
Humpel C (2011): Identifying and validating biomarkers for Alzheimer's disease. Trends Biotechnol 29:26–32.
Ibanez A, Manes F (2012): Contextual social cognition and the behavioral variant of frontotemporal dementia. Neurology 78: 1354–1362.
Ibáñez A, Kuljid RO, Matallana D, Manes F (2014): Bridging psychiatry and neurology through social neuroscience. World Psychiatry 13:148–149.
Ibáñez A, García AM, Esteves S, Yoris A, Muñoz E, Reynaldo L, Pietto ML, Adolfi F, Manes F (2016): Social neuroscience:

Undoing the schism between neurology and psychiatry. Soc Neurosci, doi:10.1080/17470919.2016.1245214.

Irish M, Piguet O, Hodges JR, Hornberger M (2014): Common and unique gray matter correlates of episodic memory dysfunction in frontotemporal dementia and Alzheimer's disease. Hum Brain Mapp 35:1422–1435.

Li Y, Qin Y, Chen X, Li W (2013): Exploring the functional brain network of Alzheimer's disease: based on the computational experiment. PloS One 8:e73186.

Liu Z, Zhang Y, Yan H, Bai L, Dai R, Wei W, Zhong C, Xue T, Wang H, Feng Y, You Y, Zhang X, Tian J (2012): Altered topological patterns of brain networks in mild cognitive impairment and Alzheimer's disease: a resting-state fMRI study. Psychiatry Res 202:118–125.

Lu PH, Mendez MF, Lee GJ, Leow AD, Lee HW, Shapira J, Jimenez E, Boeve BB, Caselli RJ, Graff-Radford NR, Jack CR, Kramer JH, Miller BL, Bartzokis G, Thompson PM, Knopman DS (2013): Patterns of brain atrophy in clinical variants of frontotemporal lobar degeneration. Dement Geriatr Cogn Disord 35:34–50.

Maris E, Oostenveld R (2007): Nonparametric statistical testing of EEG- and MEG-data. J Neurosci Methods 164:177–190.

McKhann GM, Knopman DS, Chertkow H, Hyman BT, Jack CR, Jr., Kawas CH, Klunk WE, Koroshetz WJ, Manly JJ, Mayeux R, Mohs RC, Morris JC, Rossor MN, Scheltens P, Carrillo MC, Thies B, Weintraub S, Phelps CH (2011): The diagnosis of dementia due to Alzheimer's disease: recommendations from the National Institute on Aging-Alzheimer's Association workgroups on diagnostic guidelines for Alzheimer's disease. Alzheimers Dement 7:263–269.

Melloni M, Billeke P, Baez S, Hesse E, de la Fuente L, Forno G, Birba A, Garcia-Cordero I, Serrano C, Plastino A, Slachevsky A, Huepe D, Sigman M, Manes F, Garcia AM, Sedeno L, Ibanez A (2016): Your perspective and my benefit: multiple lesion models of self-other integration strategies during social bargaining. Brain. 139:3022–3040.

Menon V (2011): Large-scale brain networks and psychopathology: a unifying triple network model. Trends Cognit Sci 15: 483–506.

Nichols TE, Holmes AP (2002): Nonparametric permutation tests for functional neuroimaging: a primer with examples. Hum Brain Mapp 15:1–25.

Oostenveld R, Fries P, Maris E, Schoffelen JM (2011): FieldTrip: Open source software for advanced analysis of MEG, EEG, and invasive electrophysiological data. Comput Intell Neurosci 2011:156869.

Papo D, Zanin M, Pineda-Pardo JA, Boccaletti S, Buldu JM (2014): Functional brain networks: great expectations, hard times and the big leap forward. Philos Trans R Soc Lond B Biol Sci 369. doi:10.1098/rstb.2013.0525.

Pievani M, de Haan W, Wu T, Seeley WW, Frisoni GB (2011): Functional network disruption in the degenerative dementias. Lancet. Neurol 10:829–843.

Pievani M, Filippini N, van den Heuvel MP, Cappa SF, Frisoni GB (2014): Brain connectivity in neurodegenerative diseases–-from phenotype to proteinopathy. Nat Rev Neurol 10: 620–633.

Piguet O, Hornberger M, Mioshi E, Hodges JR (2011a): Behavioural-variant frontotemporal dementia: diagnosis, clinical staging, and management. Lancet Neurol 10:162–172.

Piguet O, Petersen A, Yin Ka Lam B, Gabery S, Murphy K, Hodges JR, Halliday GM (2011b): Eating and hypothalamus changes in behavioral-variant frontotemporal dementia. Ann Neurol 69:312–319.

Prince, M., Wimo, A., Guerchet, M., Gemma-Claire, A., Wu, Y.T., Prina, M. 2015. World Alzheimer Report 2015: The Global Impact of Dementia - An analysis of prevalence, incidence, cost and trends.

Rabinovici GD, Seeley WW, Kim EJ, Gorno-Tempini ML, Rascovsky K, Pagliaro TA, Allison SC, Halabi C, Kramer JH, Johnson JK, Weiner MW, Forman MS, Trojanowski JQ, Dearmond SJ, Miller BL, Rosen HJ (2007): Distinct MRI atrophy patterns in autopsy-proven Alzheimer's disease and frontotemporal lobar degeneration. Am J Alzheimers Dis Other Demen 22:474–488.

Rascovsky K, Hodges JR, Knopman D, Mendez MF, Kramer JH, Neuhaus J, van Swieten JC, Seelaar H, Dopper EG, Onyike CU, Hillis AE, Josephs KA, Boeve BF, Kertesz A, Seeley WW, Rankin KP, Johnson JK, Gorno-Tempini ML, Rosen H, Prioleau-Latham CE, Lee A, Kipps CM, Lillo P, Piguet O, Rohrer JD, Rossor MN, Warren JD, Fox NC, Galasko D, Salmon DP, Black SE, Mesulam M, Weintraub S, Dickerson BC, Diehl-Schmid J, Pasquier F, Deramecourt V, Lebert F, Pijnenburg Y, Chow TW, Manes F, Grafman J, Cappa SF, Freedman M, Grossman M, Miller BL (2011): Sensitivity of revised diagnostic criteria for the behavioural variant of frontotemporal dementia. Brain 134:2456–2477.

Reijneveld JC, Ponten SC, Berendse HW, Stam CJ (2007): The application of graph theoretical analysis to complex networks in the brain. Clin Neurophysiol 118:2317–2331.

Rubinov M, Sporns O (2010): Complex network measures of brain connectivity: uses and interpretations. NeuroImage 52: 1059–1069.

Sanabria-Diaz G, Martinez-Montes E, Melie-Garcia L, Alzheimer's Disease Neuroimaging I (2013): Glucose metabolism during resting state reveals abnormal brain networks organization in the Alzheimer's disease and mild cognitive impairment. PloS One 8:e68860.

Santamaria-Garcia H, Reyes P, Garcia A, Baez S, Martinez A, Santacruz JM, Slachevsky A, Sigman M, Matallana D, Ibanez A (2016): First symptoms and neurocognitive correlates of behavioral variant frontotemporal dementia. J Alzheimers Dis 54: 957–970.

Sanz-Arigita EJ, Schoonheim MM, Damoiseaux JS, Rombouts SA, Maris E, Barkhof F, Scheltens P, Stam CJ (2010): Loss of 'small-world' networks in Alzheimer's disease: graph analysis of FMRI resting-state functional connectivity. PloS One 5:e13788.

Sedeno L, Couto B, Garcia-Cordero I, Melloni M, Baez S, Morales Sepulveda JP, Fraiman D, Huepe D, Hurtado E, Matallana D, Kuljis R, Torralva T, Chialvo D, Sigman M, Piguet O, Manes F, Ibanez A (2016): Brain network organization and social executive performance in frontotemporal dementia. J Int Neuropsychol Soc 22:250–262.

Seeley WW, Crawford RK, Zhou J, Miller BL, Greicius MD (2009): Neurodegenerative diseases target large-scale human brain networks. Neuron 62:42–52.

Seo EH, Lee DY, Lee JM, Park JS, Sohn BK, Choe YM, Byun MS, Choi HJ, Woo JI (2013a): Influence of APOE genotype on whole-brain functional networks in cognitively normal elderly. PloS One 8:e83205.

Seo EH, Lee DY, Lee JM, Park JS, Sohn BK, Lee DS, Choe YM, Woo JI (2013b): Whole-brain functional networks in cognitively normal, mild cognitive impairment, and Alzheimer's disease. PloS One 8:e53922.

Shaw LM, Korecka M, Clark CM, Lee VM, Trojanowski JQ (2007): Biomarkers of neurodegeneration for diagnosis and monitoring therapeutics. Nat Rev Drug Discov 6:295–303.

Sporns O (2014): Contributions and challenges for network models in cognitive neuroscience. Nat Neurosci 17:652–660.

Stam CJ, Jones BF, Nolte G, Breakspear M, Scheltens P (2007): Small-world networks and functional connectivity in Alzheimer's disease. Cereb Cortex 17:92–99.

Supekar K, Menon V, Rubin D, Musen M, Greicius MD (2008): Network analysis of intrinsic functional brain connectivity in Alzheimer's disease. PLoS Comput Biol 4:e1000100.

Telesford QK, Burdette JH, Laurienti PJ (2013): An exploration of graph metric reproducibility in complex brain networks. Front Neurosci 7:67.

Telesford QK, Simpson SL, Burdette JH, Hayasaka S, Laurienti PJ (2011): The brain as a complex system: using network science as a tool for understanding the brain. Brain Connectivity 1:295–308.

Tijms BM, Wink AM, de Haan W, van der Flier WM, Stam CJ, Scheltens P, Barkhof F (2013): Alzheimer's disease: connecting findings from graph theoretical studies of brain networks. Neurobiol Aging 34:2023–2036.

Torralva T, Roca M, Gleichgerrcht E, Bekinschtein T, Manes F (2009): A neuropsychological battery to detect specific executive and social cognitive impairments in early frontotemporal dementia. Brain 132:1299–1309.

Tzourio-Mazoyer N, Landeau B, Papathanassiou D, Crivello F, Etard O, Delcroix N, Mazoyer B, Joliot M (2002): Automated anatomical labeling of activations in SPM using a macroscopic anatomical parcellation of the MNI MRI single-subject brain. NeuroImage 15:273–289.

van den Heuvel MP, Stam CJ, Boersma M, Hulshoff Pol HE (2008): Small-world and scale-free organization of voxel-based resting-state functional connectivity in the human brain. NeuroImage 43:528–539.

van Wijk BC, Stam CJ, Daffertshofer A (2010): Comparing brain networks of different size and connectivity density using graph theory. PloS One 5:e13701.

Wang J, Zuo X, Dai Z, Xia M, Zhao Z, Zhao X, Jia J, Han Y, He Y (2013): Disrupted functional brain connectome in individuals at risk for Alzheimer's disease. Biol Psychiatry 73:472–481.

Watts DJ, Strogatz SH (1998): Collective dynamics of 'small-world' networks. Nature 393:440–442.

Whitwell JL, Josephs KA, Avula R, Tosakulwong N, Weigand SD, Senjem ML, Vemuri P, Jones DT, Gunter JL, Baker M, Wszolek ZK, Knopman DS, Rademakers R, Petersen RC, Boeve BF, Jack CR Jr (2011): Altered functional connectivity in asymptomatic MAPT subjects: a comparison to bvFTD. Neurology 77: 866–874.

Whitwell JL, Przybelski SA, Weigand SD, Ivnik RJ, Vemuri P, Gunter JL, Senjem ML, Shiung MM, Boeve BF, Knopman DS, Parisi JE, Dickson DW, Petersen RC, Jack CR, Jr, Josephs KA (2009): Distinct anatomical subtypes of the behavioural variant of frontotemporal dementia: a cluster analysis study. Brain 132:2932–2946.

Xiang J, Guo H, Cao R, Liang H, Chen J (2013): An abnormal resting-state functional brain network indicates progression towards Alzheimer's disease. Neural Regen Res 8:2789–2799.

Yao Z, Zhang Y, Lin L, Zhou Y, Xu C, Jiang T, Alzheimer's Disease Neuroimaging I (2010): Abnormal cortical networks in mild cognitive impairment and Alzheimer's disease. PLoS Comput Biol 6:e1001006.

Zalesky A, Fornito A, Bullmore ET (2010): Network-based statistic: identifying differences in brain networks. NeuroImage 53: 1197–1207.